



International Journal of Pharmacology

ISSN 1811-7775



Research Article

Simvastatin Loaded D- α -tocopherol Polyethylene Glycol 1000 Succinate Micelles Augments Cytotoxicity Against Breast Cancer Cells

^{1,2}Gamal A. Shazly, ^{3,4}Gehan M. Elossaily, ¹Mohamed A. Ibrahim, ⁵Omar S. Aljohani, ⁶Usama A. Fahmy and ¹Kazi Mohsin

¹Department of Pharmaceutics, College of Pharmacy, King Saud University, P.O. Box 2457, Riyadh 11451, Saudi Arabia

²Department of Industrial Pharmacy, College of Pharmacy, Assiut University, Assiut, Egypt

³Department of Pathology, Faculty of Medicine, Almaarefa University for Science and Technology, Riyadh, Saudi Arabia

⁴Department of Pathology, Faculty of Medicine, Assiut University, Assiut, Egypt

⁵Department of natural products and alternative medicine, Faculty of Pharmacy, King Abdulaziz University, Jeddah 21542, Saudi Arabia

⁶Department of Pharmaceutics, Faculty of Pharmacy, King Abdulaziz University, Jeddah 21542, Saudi Arabia

Abstract

Background and Objective: Statins are antihyperlipidemic drugs which reported with its high cytotoxicity. Micelles are identified for their potential in drug delivery of cytotoxic agents. Thus, the purpose of this study was to determine the potential enhancement of simvastatin cytotoxicity activity in MCF-7 breast cancer cells via its formulation in micelles. **Materials and Methods:** Simvastatin was formulated in micelles using a thin-film hydration technique. Particle size, shape, and release studies were used to characterize the formula. **Results:** Simvastatin micelles exhibited enhanced *in vitro* drug release. Further, it exhibited enhanced cytotoxicity against breast cancer cells. Cell cycle analysis indicated the accumulation of cells challenged with simvastatin micelles in G2/M and pre-G1 phases. Staining of cells with annexin V indicated a significant elevation of percentage cells with early and late apoptosis as well as total cell death. Besides, the formulation significantly disturbed mitochondrial membrane potential and cellular content of caspase 3. Besides, the intracellular release of Reactive Oxygen Species (ROS) was enhanced by simvastatin micelles. **Conclusion:** The prepared formula of simvastatin significantly potentiates its cytotoxic activities against MCF-7 cells. This is mediated, at least partly, by enhanced simvastatin cellular permeation and apoptosis.

Key words: Simvastatin, cytotoxicity, breast cancer, TPGS, apoptosis, micelles, thin-film hydration technique

Citation: Gamal A. Shazly, Gehan M. Elossaily, Mohamed A. Ibrahim, Omar S. Aljohani, Usama A. Fahmy and Kazi Mohsin, 2020. Simvastatin loaded D- α -tocopherol polyethylene glycol 1000 succinate micelles augments cytotoxicity against breast cancer cells. *Int. J. Pharmacol.*, 16: 492-499.

Corresponding Author: Usama A. Fahmy, Department of natural products and alternative medicine, Faculty of Pharmacy, King Abdulaziz University, Jeddah 21542, Saudi Arabia

Copyright: © 2020 Gamal A. Shazly *et al.* This is an open access article distributed under the terms of the creative commons attribution License, which permits unrestricted use, distribution and reproduction in any medium, provided the original author and source are credited.

Competing Interest: The authors have declared that no competing interest exists.

Data Availability: All relevant data are within the paper and its supporting information files.

INTRODUCTION

Statins are antihyperlipidemic drugs that inhibit the pathway of cholesterol biosynthesis. Statins are 3-hydroxy-3-methylglutaryl coenzyme A (HMGCoA) reductase inhibitors. Cholesterol is essential for cell membrane structure, hormones, vitamin D and other physiological processes¹⁻³. Statins are key for reducing the incidence of cardiovascular disease³⁻⁵. On the other hand, compounds that contribute to the depletion of cholesterol from the body affect various cellular events. Statins inhibit cholesterol synthesis through the inhibition of HMG-CoA reductase. The reductase enzyme is responsible for catalyzing HMG-CoA conversion to mevalonate.

The role of statins is not restricted to their lipid-lowering effects, reports have shown statins improve endothelial function, immune modulation, antioxidant activity, anti-inflammatory and can be used as anti-cancer drugs⁶⁻⁹. These properties, along with a high safety profile, have made statins more appealing and continue to be a commonly prescribed medication. The statin's other cholesterol-independent or pleiotropic effects are related to cellular proliferation and differentiation¹⁰⁻¹². Previous reports have indicated statins were to reduce proliferation and induce apoptosis in several cancer cells¹³⁻¹⁵.

Simvastatin (SMV) is one of the most frequently prescribed statin drugs to treat hyperlipidemia^{3,16}. Reports have indicated the chemo-preventive effects of SMV^{1,11,17,18}. SMV inhibits cancer cell growth, metastasis, angiogenesis and induce apoptosis¹⁹⁻²². SMV reduces the levels of the isoprenoid intermediates Farnesyl Diphosphate (FPP) and Geranylgeranyl Diphosphate (GGPP) which are critical for post-translational modification of the intracellular G-proteins that are essential for gene transcription involved in cell proliferation and apoptosis^{13,23}.

Micellar systems are important for solubility enhancement, controlled drug delivery and drug targeting. D- α -tocopherol polyethylene glycol 1000 succinate (vitamin E TPGS or TPGS) is a natural hydrophobic (water-insoluble) vitamin E (α -tocopherol) conjugated with the hydrophilic (water-soluble) polyethylene glycol 1000. TPGS is nonionic and widely used in drug delivery as polymeric micelles for solubilization and absorption enhancement in drug formulations²⁴⁻²⁷. TPGS was used formulation and delivery of anticancer drug paclitaxel²⁸. TPGS acts as a stabilizing factor, contributing significantly to the stability of TPGS-coated structures, such as nanoparticles^{29,30}. Also, TPGS has shown enhancement of drug transport across biological membrane barriers such as brain endothelium and to modify biological

response by inhibiting P-glycoprotein (P-gp) that is responsible for decreasing efflux of the drugs from the cells³¹. Based on the above, this study aimed to investigate the augmentation effect of TPGS polymeric micelles on the function of SMV in cancer cell growth inhibition, which shows the drug's ability to induce apoptosis. The study investigates the cytotoxicity of SMV against breast cancer cells MCF-7. Particle size, shape, and release studies were used to characterize the prepared SMV-TPGS formula.

MATERIALS AND METHODS

Study area: Part of this study was carried out in the Faculty of Pharmacy, King Abdulaziz University, Saudi Arabia, and the other part was carried out in the National Cancer Institute, Cairo University, Egypt during the period between 2018-2020.

Drug and chemicals: SMV was a kind gift from Jamjoom pharmaceuticals (Jeddah, Saudi Arabia), Vitamin E TPGS and Ethanol were purchased from Sigma Aldrich (MO, USA).

Preparation of SMV-TPGS: SMV loaded TPGS micelles were prepared by thin-film hydration method³². Firstly, SMV and TPGS (1:10 w/w ratio) were dissolved in ethanol. The ethanolic solution was evaporated by a rotary evaporator (BÜCHI Labortechnik AG, Flawil, Switzerland) to form SMV-TPGS thin film. The formed film was then hydrated water to form SMV-TPGS micelles. After that, the dispersion was centrifuged at 30,000 rpm at 4°C for 45 min. The supernatant was filtered, and the residue was lyophilized for 48 h and stored at -20°C.

Encapsulation efficiency: SMV encapsulation within SMV-TPGS micelles was determined by dissolving in ethanol then diluted with mobile phase (water: methanol: acetonitrile: orthophosphoric acid (60:30:10:1)). SMV was analyzed by a modified reversed-phase HPLC method⁵. HPLC column (250×4.6 mm i.d. Symmetry-C18, 5 μ m column) with a flow rate of 1.0 mL min⁻¹ at 25°C and an injection sample volume of 10 μ L. The detection wavelength was at λ_{max} 262 nm. Following formula is used for calculation of SMV encapsulation efficiency:

$$\text{SMV encapsulation efficiency (\%)} = \frac{\text{SMV weight micelles}}{\text{Weight of SMV feed}} \times 100$$

Vesicle size measurement: SMV-TPGS vesicle size was determined by dynamic light scattering technique (DLS) using Malvern Zetasizer Nano ZSP, Malvern Panalytical Ltd (Malvern,

United Kingdom). The investigated samples were dispersed in deionized water before measurements of the size. Data represent the average of five measurements³³.

Transmission electron microscopy: Transmission electron microscope JEOL-JEM-1011 (JEOL-Tokyo, Tokyo, Japan) was used to explore the prepared SMV-TPGS micelles. The micelles sample was suspended in distilled water and one drop of the sample was spread on a carbon-coated grid. Also, 1% phosphotungstic acid was used for negative staining of the sample. Then, the sample was dried at ambient temperature for 15 min before visualization³³.

In vitro drug release of SMV-TPGS micelles: The prepared SMV-TPGS micelles were assessed for SMV release by dialysis bag method²⁰. SMV-TPGS micelles (equivalent to 2 mg of SMV) were placed in a dialysis bag (12 kDa cut off) and then submerged into phosphate buffer saline (pH 7.4) with stirring at 100 rpm at 37°C. At each time interval, 5 mL of sample was withdrawn and SMV concentration was determined by the HPLC method as discussed earlier³⁴.

Cell culture and determination of IC₅₀ using MTT assay: MCF-7 were cultured in Roswell Park Memorial Institute (RPMI) Medium 1640 (1×) supplemented with 10% fetal calf serum (FCS), 1X non-essential amino acids (Sigma-Aldrich, Irvine, UK), 100 µL mL⁻¹ (v/v) penicillin-streptomycin, 1 mM sodium pyruvate (Sigma-Aldrich), and 1 µL mL⁻¹ bovine insulin (Sigma-Aldrich). MCF-7 Cell lines were maintained in a humidified incubator at 37°C with 5% CO₂. Cells were passaged using 0.05% trypsin-Ethylenediaminetetraacetic acid (EDTA) (1×). All experiments were carried out with cell lines no more than 10 passages apart to ensure biological repeats and limit the mutational effect of passaging. Cell lines were not synchronized before experimentation. For determining IC₅₀ values, 1×10⁵ cells were seeded into a 96-well plate. The seeded MCF-7 cells were then incubated for 24 h at 37°C in a 5% CO₂ incubator. The cells were then incubated with SMV-M, SMV-raw, and plain-M for 24 h. Different samples equivalent to different concentrations of SMV ranging from 0.1 to 1000 µM were tested. IC₅₀ values were determined using Thiazolyl Blue Tetrazolium Bromide (MTT) assay using a commercially available kit (ABCAM, Cambridge, UK). The experiments were carried out in triplicate³².

Cell cycle analysis: Cell cycle analysis was studied by flow cytometry experiments following reported method³⁵. The cells were incubated with the samples: SMV-TPGS micelles formula (SMV-M), SMV-raw, and blank TPGS micelles formula (plain-M).

A control sample with cells alone was also included in the study. The samples were incubated for 24 h. After incubation with the samples, separation of cells was carried out by centrifuging the samples. The cells were then fixed with 70% cold ethanol. The cells were again separated by centrifugation and their washing was carried out with PBS buffer. The cells were then stained using propidium iodide (in PBS buffer) and RNase staining buffer before carrying out flow cytometry analysis.

Annexin V staining: The dual staining technique was performed to assess apoptosis as previously published. Cells were incubated with the samples, SMV-M, SMV-raw, and plain-M in a 6-well plate with a cell density of 1×10⁵ cells per well. A control sample with cells alone was also included in the study. The staining was carried out using a commercially available kit (BD Bioscience, San Jose, CA, USA). After incubation for 24 h, the cells were collected by centrifugation. The cells were then resuspended in 500 µL of 1X binding buffer. Then, 5 µL each of Annexin V-Fluorescein isothiocyanate Fluorescein FITC and propidium iodide (BD Bioscience) was added and incubated at room temperature for 5 min in the dark. Flow cytometry (FACS Calibur, BD Bioscience) was carried out for the analysis. The data were studied using the Multicycle software (Phoenix Flow Systems, San Diego, CA, USA)³⁶.

Caspase-3 assay: The caspase-3 content of the SMV-M was determined using a ready-to-use kit available commercially (BD Biosciences). For evaluation of the caspase-3 activity, the MCF-7 cells (5×10⁴ cells per well) were incubated with the samples. SMV-M, SMV-raw, and plain-M. A control was studied along with a control sample with cells alone. Caspase-3 content in the samples was determined by assessing the absorbance of the cell lysate at 405 nm³³.

Statistical analysis: Data are presented as the Mean±SD. Statistical tests were carried out using IBM SPSS® statistics software, version 25 (SPSS Inc., Chicago, IL, USA). Analysis of Variance (ANOVA) followed by Tukey's post hoc test was used to compare means. p<0.05 indicated statistical significance.

RESULTS

Preparation and characterization of SMV-TPGS micelles: Particle size results of the prepared SMV-TPGS formulation showed average vesicle size of (75±9.2 nm) as measured by Zetasizer Nano ZSP. TEM micrograph of the prepared SMV-TPGS micelles (Fig. 1) further confirmed the particle size

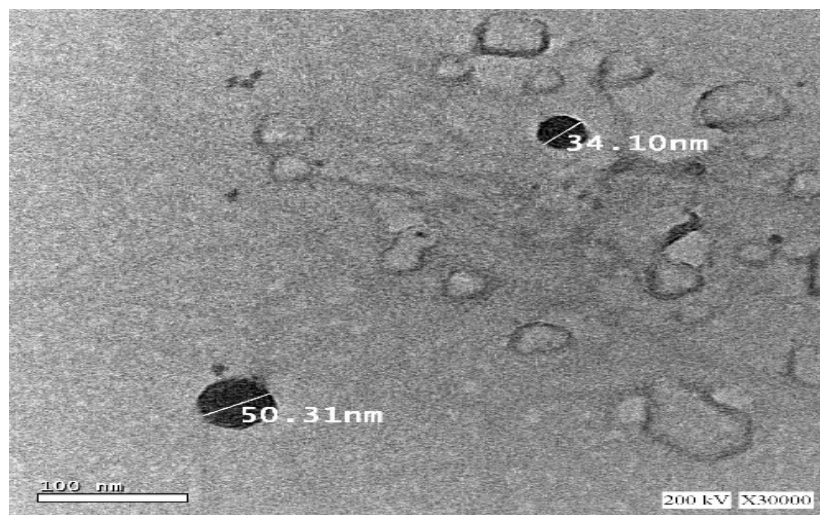


Fig. 1: Transmission electron microscope image of SMV-TPGS micelles ($\times 30,000$)

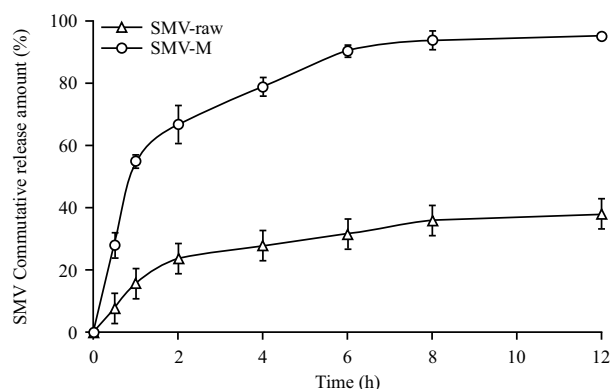


Fig. 2: *In vitro* release profile of SMV-M compared to SMV-raw in phosphate-buffered saline (PBS) buffer pH 7.4 at $37 \pm 0.5^\circ\text{C}$

Results are presented as Mean \pm SD, n = 3

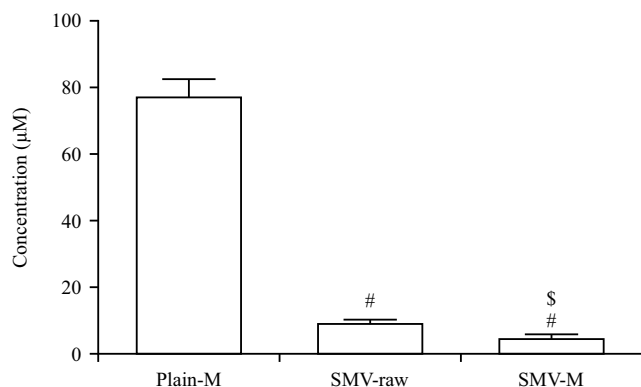


Fig. 3: Cytotoxicity of SMV-M in MCF-7 cells

#Significantly different from plain-M at $p < 0.05$, \$Significantly different from SMV-raw at $p < 0.05$

analysis result obtained by the dynamic light scattering technique. The micelle vesicles appeared nearly spherical. The smaller particle size observed in the TEM image in comparing with SMV-TPGS micelles measured by Zetasizer Nano ZSP is attributed to drying process during TEM imaging which lead to shrinkage of the micelles.

***In vitro* Release of SMV-TPGS formula:** The *in vitro* release profile of raw-SMV and optimized SMV-M is shown in Figure 2. It was evident that micelles could enhance the dissolution of SMV. Although a burst release of SMV was observed in both profiles, the release was much higher from the raw SMV. After 2 h, around 70% of SMV was released from micelles, whereas the release of the SMV-raw was around 20%. Thus, at 2 h, the drug release was more than double from the micelles as compared to the SMV-raw. At the end of 12 h, SMV release was almost complete from micelles compared to SMV-raw release of only 65%.

Determination of IC_{50} values: The IC_{50} values obtained for the samples are shown in Fig. 3. SMV-M had the least IC_{50} value which amounted to $4.87 \mu\text{M}$, whereas SMV-raw had an IC_{50} value of $9.34 \mu\text{M}$. Thus, there was a reduction to about half of the IC_{50} value of SMV when loaded in the micelles.

Cell cycle analysis: The results of cell cycle analysis are shown in Fig. 4. A significant difference in the cell cycle was observed. From the observations, the SMV-TPGS micelles (SMV-M) was found to perform as expected in all phases. There was no significant effect of plain-M on the G0-G1 phase. The percent

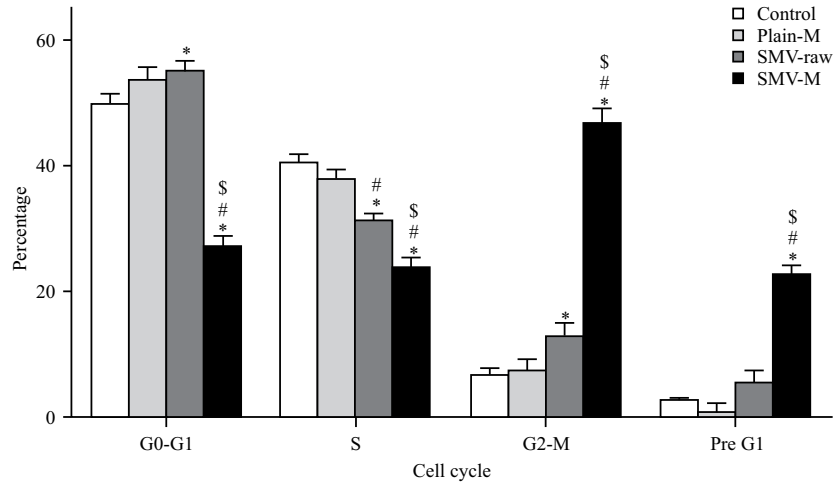


Fig. 4: Flow cytometry analysis results for cell cycle analysis

*Significantly different from control at $p < 0.05$, #Significantly different from plain-M at $p < 0.05$, §Significantly different from SMV-raw at $p < 0.05$

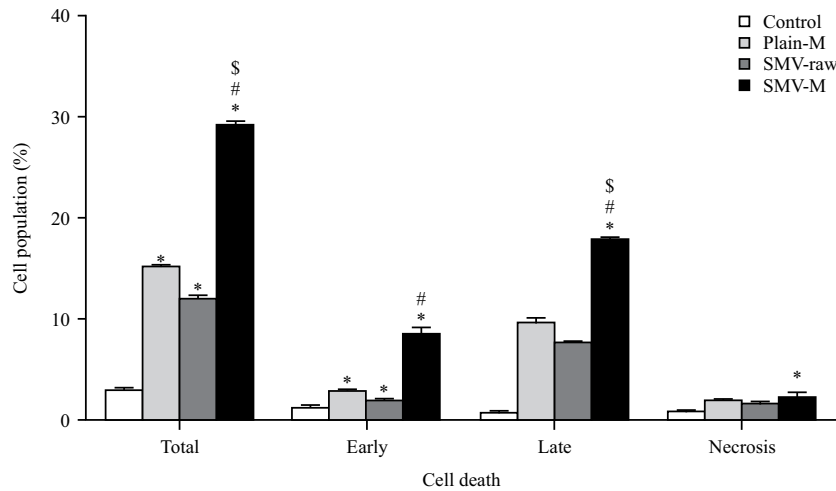


Fig. 5: Assessment of MCF-7 cell death using flow cytometric analysis after annexin V staining

*Significantly different from control at $p < 0.05$, #Significantly different from plain-M at $p < 0.05$, §Significantly different from SMV-raw at $p < 0.05$

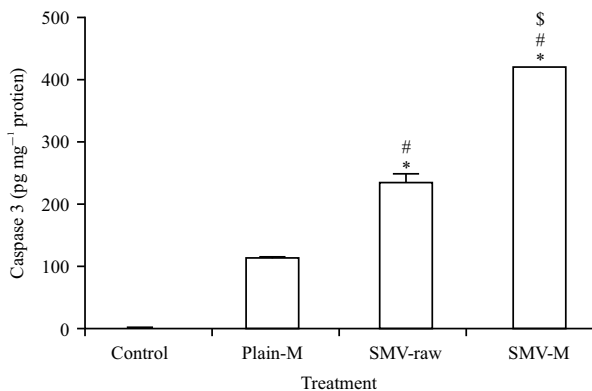


Fig. 6: Effect of SMV-M on caspase-3 content in MCF-7 cells

*Significantly different from control at $p < 0.05$, #Significantly different from plain-M at $p < 0.05$, §Significantly different from SMV-raw at $p < 0.05$

of cells in the G2-M phase showed marked enhancement on incubation with SMV-M. These effects were more significant than other samples. A similar effect was observed with pre-G1 apoptosis.

Annexin V staining: Annexin V-FITC apoptosis detection kit was used to study the apoptosis determination by flow cytometry. Figure 5 shows that SMV-M exhibited a distinct and much higher early, late, and total cell apoptosis as well as necrotic cell death when compared with other treatments.

Caspase-3 assay: The data in Fig. 6 indicate that SMV-M caused a significant enhancement in caspase-3 content amounting to an approximately two-fold increase from that of

the SMV-raw-treated cells. Also, Plain-M induces caspase-3 content as compared to control value.

DISCUSSION

Our data indicated that both SMV-raw and SMV -M possess the potent antiproliferative activity and in this regard SMV -M showed significant potentiation of SMV cytotoxicity against MCF-7 cells. In general, statins were shown to inhibit the mevalonate pathway³⁴. This leads to the mevalonate pathway intermediates, farnesyl pyrophosphate and geranylgeranyl pyrophosphate, to be depleted³⁷⁻³⁹. The depletion of mevalonate pathway intermediates leads to the disturbance of Rho protein prenylation and this disruption could explain the cytotoxic effects²¹. The outcome of this study showed similar findings with the previously reported investigations for SMV cytotoxicity. These reports include investigation of SMV cytotoxic effects against myeloma U266 cells^{40,41}, the breast cancer 47D, SKBR3 and MCF-7 cells^{1,42,43}, prostate PC-3 cells⁴⁴ and green monkey kidney GMK cells⁴⁴.

Cell cycle phase analyses of results revealed that MCF-7 cells treated with either SMV- raw or SMV-M showed a significant accumulation in G2 M and pre-G phases. This accumulation indicated the proapoptotic activity of SMV. This finding in accordance with previous reports of SMV apoptotic activity in lipoma LipPD1 cells⁴⁵, osteosarcoma AXT cells²² neuroblastoma SK-N-AS cells⁴⁶ prostate cancer PC3 and DU 145 cells⁴⁵, medulloblastoma brain tumor D283 and D341 cells^{12,22,45,46}. The results of SMV (SMV- raw or SMV-M) proapoptotic activity are also confirmed by the application of annexin V staining and caspase 3 cellular content. Our results revealed a significant enhancement of early and late apoptosis as well as caspase 3 content in MCF-7 breast cancer cells. Previous studies have indicated the ability of SMV to reduce colon cancer tumors. Treatment of animals with SMV showed a reduction in tumor sizes, increased necrotic areas and increased apoptosis scores when compared to control animal groups⁴⁷⁻⁴⁹. Finally, Micelles' formulation of SMV significantly enhances its cytotoxic activities against MCF-7 cells.

CONCLUSION

The thin-film hydration technique was successfully used to formulate SMV-M with minimized vesicle size. The formulated micelles were almost spherical. *In vitro* release of SMV from micelles was markedly higher than the SMV-raw, predicting a better presentation to the tumor cells. Micelles formulation of SMV significantly enhances its cytotoxic activities against MCF-7 cells. This is mediated, at least partly,

by enhanced apoptosis as evidenced by cell cycle analysis, annexin V staining, and determination of caspase 3 which improved cytotoxicity of SMV-M.

SIGNIFICANCE STATEMENT

This study revealed the importance of TPGS micelles formula as a nanocarrier system for improved delivery and augment the effect of SMV in cancer therapy. The results indicated the improved cytotoxic effects of SMV loaded TPGS micelles when compared with raw SMV. This can be beneficial for the treatment of breast cancer with minimum side effects as SMV is approved as a safe drug. This study will shed light on researchers and oncologists to identify the importance of nano carriers in cancer therapy.

ACKNOWLEDGMENT

The authors acknowledges the Deanship of Scientific Research at King Saud University for funding this work through the Research Group Project no. RGP-VPP-139.

REFERENCES

1. Ahmed, O.A.A., K.M. Hosny, M.M. Al-Sawahli and U.A. Fahmy, 2015. Optimization of caseinate-coated simvastatin-zein nanoparticles: Improved bioavailability and modified release characteristics. *Drug Des. Dev. Ther.*, 9: 655-662.
2. Ahmed, T.A., K.M. El-Say, O.A.A. Ahmed and B.M. Aljaeid, 2019. Superiority of TPGS-loaded micelles in the brain delivery of vinpocetine via administration of thermosensitive intranasal gel. *Int. J. Nanomed.*, Volume 14: 5555-5567.
3. Ahmed, T.A., S.M. Badr-Eldin, O.A.A. Ahmed and H. Aldawsari, 2018. Intranasal optimized solid lipid nanoparticles loaded in situ gel for enhancing trans-mucosal delivery of simvastatin. *J. Drug Delivery Sci. Technol.*, 48: 499-508.
4. Aldawsari, H.M., M.A. Elfaky, U.A. Fahmy, B.M. Aljaeid, O.A. Alshareef and K.M. El-Say, 2018. Development of a fluvastatin-loaded self-nanoemulsifying system to maximize therapeutic efficacy in human colorectal carcinoma cells. *J. Drug Deliv. Sci. Technol.*, 46: 7-13.
5. Alhakamy, N.A., U.A. Fahmy, S.M. Badr-Eldin, O.A.A. Ahmed and H.Z. Asfour *et al.*, 2020. Optimized icariin phytosomes exhibit enhanced cytotoxicity and apoptosis-inducing activities in ovarian cancer cells. *Pharm.*, Vol. 12. 10.3390/pharmaceutics12040346
6. Alhakamy, N.A., U.A. Fahmy, O.A.A. Ahmed, G. Caruso and F. Caraci *et al.*, 2020. Chitosan coated microparticles enhance simvastatin colon targeting and pro-apoptotic activity. *Marine Drugs*, Vol. 18. 10.3390/md18040226

7. Ali, A. and S. Ahmed, 2018. A review on chitosan and its nanocomposites in drug delivery. *Int. J. Biol. Macromol.*, 109: 273-286.
8. Bruinsmann, F., S. Pigana, T. Aguirre, G. Souto and G. Pereira *et al.*, 2019. Chitosan-coated nanoparticles: effect of chitosan molecular weight on nasal transmucosal delivery. *Pharm.*, Vol. 11. 10.3390/pharmaceutics11020086
9. Buranrat, B., W. Suwannaloet and J. Naowaboot, 2017. Simvastatin potentiates doxorubicin activity against MCF-7 breast cancer cells. *Oncol. Lett.*, 14: 6243-6250.
10. Carlin, C.M., A.J. Peacock and D.J. Welsh, 2007. Fluvastatin inhibits hypoxic proliferation and p38 MAPK activity in pulmonary artery fibroblasts. *Am. J. Respir. Cell Mol. Biol.*, 37: 447-456.
11. Cheng, G., 2003. Apoptosis induced by simvastatin in rat vascular smooth muscle cell through Ca²⁺-calpain and caspase-3 dependent pathway. *Pharmacol. Res.*, 48: 571-578.
12. Cheng, H. Yan, X. Jia and Z. Zhang, 2016. Preparation and *in vivo/in vitro* evaluation of formononetin phospholipid/vitamin E TPGS micelles. *J. Drug Targeting*, 24: 161-168.
13. Cho, S.J., J.S. Kim, J.M. Kim, J.Y. Lee, H.C. Jung and I.S. Song, 2008. Simvastatin induces apoptosis in human colon cancer cells and in tumor xenografts, and attenuates colitis-associated colon cancer in mice. *Int. J. Cancer*, 123: 951-957.
14. Demierre, M.F., P.D.R. Higgins, S.B. Gruber, E. Hawk and S.M. Lippman, 2005. Statins and cancer prevention. *Nat. Rev. Cancer*, 5: 930-942.
15. Tsai, H.I., L. Jiang, X. Zeng, H. Chen and Z. Li *et al.*, 2018. DACHPt-loaded nanoparticles self-assembled from biodegradable dendritic copolymer polyglutamic acid-bD- α -tocopheryl polyethylene glycol 1000 succinate for multidrug resistant lung cancer therapy. *Front. Pharmacol.*, Vol. 21. 10.3389/fphar.2018.00119
16. Fahmy, U.A., 2016. Quantification of simvastatin in mice plasma by near-infrared and chemometric analysis of spectral data. *Drug Des. Dev. Ther.*, 10: 2507-2513.
17. Fahmy, U.A., O.A.A. Ahmed and N.A. Alhakamy, 2019. Augmentation of alendronate cytotoxicity against breast cancer cells by complexation with trans-activating regulatory protein. *Int. J. Pharmacol.*, 15: 731-737.
18. Fahmy, U.A. and B.M. Aljaeid, 2016. Combined strategy for suppressing breast carcinoma MCF-7 cell lines by loading simvastatin on alpha lipoic acid nanoparticles. *Expert Opin. Drug Deliv.*, 13: 1653-1660.
19. Fahmy, U.A. and B.M. Aljaeid, 2018. Tadalafil transdermal delivery with alpha-lipoic acid self nanoemulsion for treatment of erectile dysfunction by diabetes mellitus. *Int. J. Pharmacol.*, 14: 945-951.
20. Guo, Y., J. Luo, S. Tan, B.O. Otieno and Z. Zhang, 2013. The applications of vitamin E TPGS in drug delivery. *Eur. J. Pharm. Sci.*, 49: 175-186.
21. Higashi, T., H. Hayashi, Y. Kitano, K. Yamamura and T. Kaida *et al.*, 2016. Statin attenuates cell proliferative ability via TAZ (WWTR1) in hepatocellular carcinoma. *Med. Oncol.*, Vol. 33. 10.1007/s12032-016-0845-6
22. Hindler, K., C.S. Cleeland, E. Rivera and C.D. Collard, 2006. The role of statins in cancer therapy. *Oncologist*, 11: 306-315.
23. Kamel, W.A., E. Sugihara, H. Nobusue, S. Yamaguchi-Iwai, N. Onishi *et al.*, 2017. Simvastatin-induced apoptosis in osteosarcoma cells: a key role of RhoA-AMPK/p38 MAPK signaling in antitumor activity. *Mol. Cancer Ther.*, 16: 182-192.
24. Kassner, F., T. Sauer, M. Penke, S. Richter and K. Landgraf *et al.*, 2018. Simvastatin induces apoptosis in PTEN-haploinsufficient lipoma cells. *Int. J. Mol. Med.*, 41: 3691-3698.
25. Khatik, R., R. Mishra, A. Verma, P. Dwivedi and V. Kumar *et al.*, 2013. Colon-specific delivery of curcumin by exploiting Eudragit-decorated chitosan nanoparticles *in vitro* and *in vivo*. *J. Nanopart. Res.*, Vol. 15. 10.1007/s11051-013-1893-x
26. Kurakula, M., O.A.A. Ahmed, U.A. Fahmy and T.A. Ahmed, 2016. Solid lipid nanoparticles for transdermal delivery of avanafil: Optimization, formulation, *in-vitro* and *ex-vivo* studies. *J. Liposome Res.*, 26: 288-296.
27. Kuzyk, C.L., C.C. Anderson and J.R. Roede, 2020. Simvastatin induces delayed apoptosis through disruption of glycolysis and mitochondrial impairment in neuroblastoma cells. *Clin. Transl. Sci.*, 13: 563-572.
28. Lavi, R., X.Y. Zhu, A.R. Chade, J. Lin, A. Lerman and L.O. Lerman, 2010. Simvastatin decreases endothelial progenitor cell apoptosis in the kidney of hypertensive hypercholesterolemic pigs. *Arteriosclerosis Thrombosis Vasc. Biol.*, 30: 976-983.
29. Yu, X., Y. Pan, H. Ma and W. Li, 2013. Simvastatin inhibits proliferation and induces apoptosis in human lung cancer cells. *Oncol. Res. Featuring Preclinical Clin. Cancer Ther.*, 20: 351-357.
30. Prabakaran, M., 2015. Chitosan-based nanoparticles for tumor-targeted drug delivery. *Int. J. Biol. Macromol.*, 72: 1313-1322.
31. Mainardes, R.M. and R.C. Evangelista, 2005. PLGA nanoparticles containing praziquantel: Effect of formulation variables on size distribution. *Int. J. Pharm.*, 290: 137-144.
32. Fahmy, U.A. and B.M. Aljaeid, 2016. Combined strategy for suppressing breast carcinoma MCF-7 cell lines by loading simvastatin on alpha lipoic acid nanoparticles. *Expert Opin. Drug Deliv.*, 13: 1653-1660.
33. Matuszewicz, L., J. Podkalicka and A. Sikorski, 2018. Immunoliposomes with simvastatin as a potential therapeutic in treatment of breast cancer cells overexpressing HER2—An *In vitro* study. *Cancers*, Vol. 10. 10.3390/cancers10110418
34. Mauro, V.F. and J.L. MacDonald, 1991. Simvastatin: A review of its pharmacology and clinical use. *Ann. Pharmacother.*, 25: 257-264.

35. Porfire, A., D. Muntean, M. Achim, L. Vlase and I. Tomuta, 2015. Simultaneous quantification of simvastatin and excipients in liposomes using near infrared spectroscopy and chemometry. *J. Pharm. Biomed. Anal.*, 107: 40-49.
36. Jee, M.K., Y.B. Im, J.I. Choi and S.K. Kang, 2013. Compensation of cATSCs-derived TGF β 1 and IL10 expressions was effectively modulated atopical dermatitis. *Cell Death Dis.*, Vol. 4. 10.1038/cddis.2013.4
37. Radwan, M.F., M.A. El-Moselhy, U.A. Fahmy and B.M. Aljaeid, 2019. Novel combination of alprostadil-D-tocopheryl polyethylene glycol succinate for treatment of erectile dysfunction. *Int. J. Pharmacol.*, 15: 738-744.
38. Safwat, S., R.A. Ishak, R.M. Hathout and N.D. Mortada, 2017. Nanostructured lipid carriers loaded with simvastatin: Effect of PEG/glycerides on characterization, stability, cellular uptake efficiency and *in vitro* cytotoxicity. *Drug Dev. Ind. Pharm.*, 43: 1112-1125.
39. Sekine, Y., H. Nakayama, Y. Miyazawa, H. Kato and Y. Furuya *et al.*, 2018. Simvastatin in combination with meclofenamic acid inhibits the proliferation and migration of human prostate cancer PC-3 cells via an AKR1C3 mechanism. *Oncol. Lett.*, 15: 3167-3172.
40. Åberg, M., M. Wickström and A. Siegbahn, 2008. Simvastatin induces apoptosis in human breast cancer cells in a NF κ B-dependent manner and abolishes the anti-apoptotic signaling of TF/FVIIa and TF/FVIIa/FXa. *Thrombosis Res.*, 122: 191-202.
41. Sheikholeslami, K., A.A. Sher, S. Lockman, D. Kroft and M. Ganjibakhsh *et al.*, 2019. Simvastatin induces apoptosis in medulloblastoma brain tumor cells via mevalonate cascade prenylation substrates. *Cancers*, Vol. 11. 10.3390/cancers11070994
42. Tiwari, R. and K. Pathak, 2011. Nanostructured lipid carrier versus solid lipid nanoparticles of simvastatin: Comparative analysis of characteristics, pharmacokinetics and tissue uptake. *Int. J. Pharm.*, 415: 232-243.
43. Varma, M.V.S. and R. Panchagnula, 2005. Enhanced oral paclitaxel absorption with vitamin E-TPGS: Effect on solubility and permeability *in vitro*, *in situ* and *in vivo*. *Eur. J. Pharmaceut. Sci.*, 25: 445-453.
44. Wang, S.T., H.J. Ho, J.T. Lin, J.J. Shieh and C.Y. Wu, 2017. Simvastatin-induced cell cycle arrest through inhibition of STAT3/SKP2 axis and activation of AMPK to promote p27 and p21 accumulation in hepatocellular carcinoma cells. *Cell Death Dis.*, Vol. 8. 10.1038/cddis.2016.472
45. Wolpin, B.M. and R.J. Mayer, 2008. Systemic treatment of colorectal cancer. *Gastroenterol.*, 134: 1296-1310.
46. Wright, J.L., S. Zhou, O. Preobrazhenska, C. Marshall and D.D. Sin *et al.*, 2011. Statin reverses smoke-induced pulmonary hypertension and prevents emphysema but not airway remodeling. *Am. J. Respir. Crit. Care Med.*, 183: 50-58.
47. Yu, J., A. Bridgers, J. Polli, A. Vickers and S. Long *et al.*, 1999. Vitamin E-TPGS increases absorption flux of an HIV protease inhibitor by enhancing its solubility and permeability. *Pharm. Res.*, 16: 1812-1817.
48. Zidan, A.S., K.M. Hosny, O.A.A. Ahmed and U.A. Fahmy, 2016. Assessment of simvastatin niosomes for pediatric transdermal drug delivery. *Drug Deliv.*, 23: 1536-1549.
49. Alhakamy, N.A., O.A.A. Ahmed, H.M. Aldawsari, M.Y. Alfaifi, B.G. Eid, A.B. Abdel-Naim and U.A. Fahmy, 2019. Encapsulation of lovastatin in zein nanoparticles exhibits enhanced apoptotic activity in HepG2 cells. *Int. J. Mol. Sci.*, Vol. 20. 10.3390/ijms20225788